Title:	***Cosmic ray impact on NISP spectroscopic performance***
Reference :	EUCL-CPP-TN-7-002
Issue :	1.0
Date :	15/03/2013
Custodian :	A. Ealet

Authors	**Function**	**Signature and Date**
A. Ealet	NISP spectro Instrument scientist	Anne Ealet Anne Ealet (Mar 18, 2013)
A. Chapon	Detector Simulation	Arnaud Chapon Arnaud Chapon (Mar 18, 2013)
J. Zoubian	Image Pixel Simulator	Julien Zoubian (Mar 18, 2013)
K. Ganga	Radiation Scientist	Ken Ganga Ken Ganga (Mar 18, 2013)
Approved by	**Function**	**Signature and Date**
E. Prieto	NISP system engineer	Eric prieto Eric prieto (Mar 18, 2013)
A.Ealet	NISP spectro Instrument scientist	Anne Ealet Anne Ealet (Mar 18, 2013)
Authorised by	**Function**	**Signature and Date**
T. Maciaszek	NISP project manager	thierry maciaszek thierry maciaszek (Mar 18, 2013)

Document version tracking

Issue	Date	Pages	Description of changes	Comments
0.1	27/02/2013	all	Generation of document	
0.3	12/03/2013	all	Add all contributions	
1.0	15/03/2013	all	released	

Table of contents

1 Purpose of the document

This document aims to investigate the impact of cosmic rays in spectroscopic science images. To do so, the EUCLID cosmic primary and secondary spectrum of particles has been estimated. A tool to simulate their impact on NIR detector has been developed. This tool has been used inside the simulation of NISP dispersed images. This allows to study the impact of cosmic rays on the NISP image in spectroscopy and to estimate the possible science degradation with or without the cosmic degradation. A study of the needs and on requirement on the on-board cosmic rejection treatment is then derived.

2 The cosmic rate expected in EUCLID

In this section we describe the rate of cosmic rays expected at L2 for EUCLID. We use CREME96 – [https://creme.isde.vanderbilt.edu/].

2.1 Primary spectrum of particles

The expected primary spectrum of single particles in L2 is mainly composed of protons. We expect 2 kinds of contributions: the Galactic part which is an almost flat flux of very high energy protons (in the > GeV range). This contribution is almost constant during the mission; the solar particles, which have a rate, which depends of the solar activity, and have in general, lower energies. We consider minimum and maximum solar activities periods, which alternate by a period of roughly 11 years.

2.1.1 Galactic contribution

This contribution is shown on Figure 1 in blue and red depending on solar activity. While the peak is broad, most of the particles from the Galaxy are in the GeV range. Even a small amount of shielding removes a large amount of low energy cosmic rays. There is little benefit to much more than a couple of millimeters of shielding, as far as Galactic cosmic rays are concerned. Note that some 90% of the particles are simply protons. Heavier ions make up the other 10%.

2.1.2 Solar contribution

Solar Flare periods are dominated by particles in the 1-10 MeV range. Since these low-energy particles deposit roughly the same amount of energy as higher energy, Galactic particles, and there are far more of them, even if they are emitted only during brief periods, most of the total damage to the detectors or electronics that ultimately comes from particle hits will be caused by these ~MeV particles emitted during solar flares.

2.1.3 Global expected spectrum

Figure 1 shows these contributions of particle during the different periods of solar activity [from CREME96 --https://creme.isde.vanderbilt.edu/]. The red curves correspond to maxima in solar activity. The blue curves correspond to solar minima.
The grey curves correspond to solar flare periods, with the lowest grey curves corresponding to the worst week-long solar flare averages, the middle curves corresponding to the worst day-long averages, and the top curves corresponding to the worst five-minute period. Note that during "normal" periods, Galactic cosmic rays dominate the flux.

At low to intermediate energies, the fluxes are inversely proportional to the amount of solar activity, as during these periods the Sun's magnetic field grows and "shields" the Earth more. During solar flares, we are shielded even more by the Sun's magnetic field, but in this case the flux of particles emitted by the Sun itself increases enormously, yielding the gray curves.

A small amount of material can stop low energy protons and other ions. For each solar activity class (low activity, high activity, solar flare, etc.), we show a solid line, a dashed line, and a dotted line. The solid line corresponds to the flux without shielding. The dashed line corresponds to 2 mm of Aluminum shielding, and the dotted line corresponds to 3 cm of shielding. We can see than after 2 mm of Al shielding, we are left with only the high energy particles.

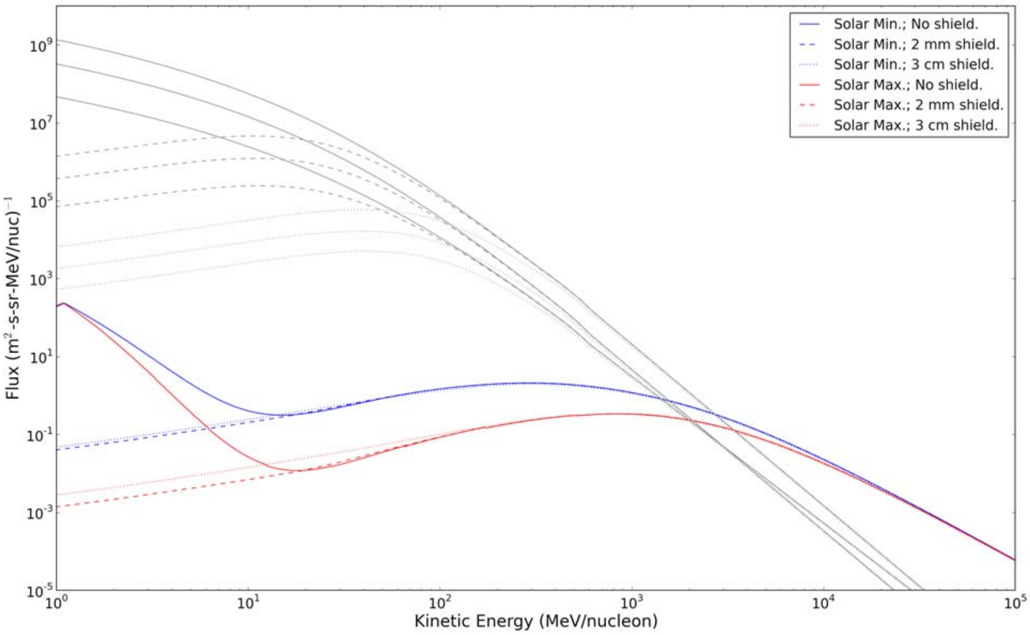

Figure 1: Primary spectra of particles from galactic and solar contributions expected in L2 as a function of energy . at solar minima (blue) and maxima (red) are shown with the effect of different shielding wth dashes.

2.1.4 Euclid expected rate

Integrating the curves in the spectrum above yields the following number of hits:

Event/cm^2/s	None	100 mils (~ 2.5 mm Al)	1000 mils (~2.5 cm Al)
Solar Min	4.7	4.4	4.2
Solar Max	1.7	1.6	1.5
Worst week	140000	11000	980
Worst day	910000	52000	3000
Worst 5 mn	3700000	190000	11000

The units are events/cm-squared/s. Note that 100 mils is about 2.5 mm of aluminum, and 1000 mils would be about 2.5 cm . The basic conclusion is that we will expect of order five particles/cm^2/second or less during "normal" periods (i.e., outside of solar flares), though this number can increase by many orders of magnitude during solar flares. It is evident, that during solar flares, we cannot accommodate any science evaluation. The case of solar flares is then not investigated later on in this document and in the code discussed below, we will use 5 events/cm-squared/s.

2.2 Secondary particles

The primary spectrum of particles described above does not take into account secondary particles, which are generated by interaction of the primary protons in the environment of the instrument itself.

To do so, we build a GEANT4 simulation, which is a toolkit for the simulation of the passage of particles through matter. It is commonly used in many areas of application including high energy physics, nuclear physics and space science.

2.2.1 NISP geometry

The full payload module has been roughly described as input of the GEANT4 geometry, as shown on Figure 2.

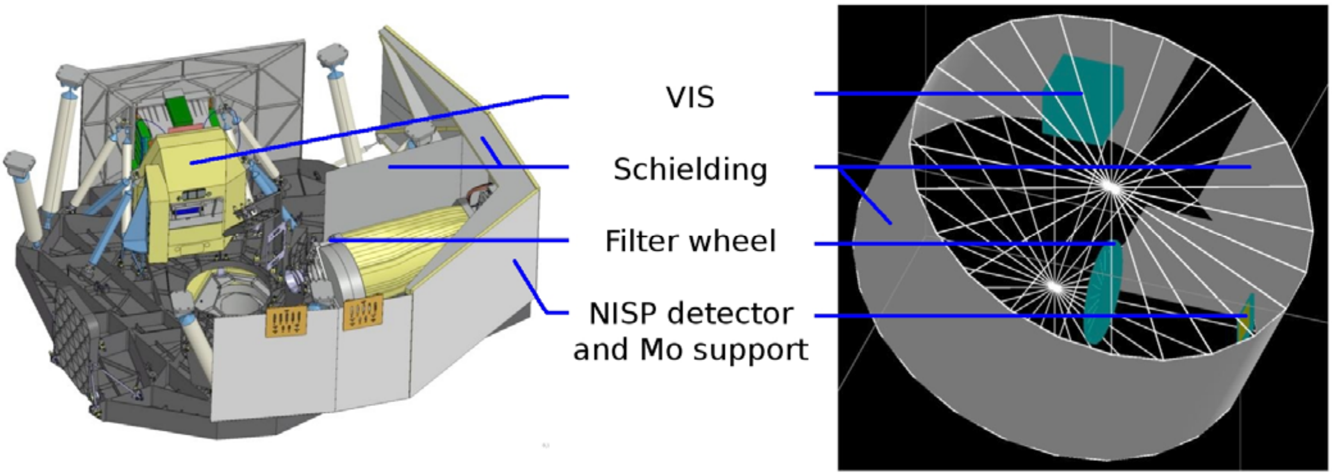

Figure 2: Geometry definition of the payload module

NISP detectors are specified with a 7 µm thickness of HgCdTe, fixed on a support made in molybdenum which is 1cm thick. Shielding has been considered as a tube of 5mm SiC at the top and 2mm aluminium at the bottom. The wheels are SiC cylinders of 50 cm diameter and 1cm thick. The VIS instrument is a box of 30 cm in SiC
Currently, the far elements of the NISP instrument and telescope geometry are not known with a very precise geometry definition and this can be refined when we have more information.

2.2.2 Geant 4 simulation

Mono-energetic protons have been generated with random momentums and tracked through matter. They can produce secondary's particles by multiple scattering, ionization, bremsstrahlung or pair production. Secondaries are also tracked in GEANT4 and can be detected if they have an interaction in the NISP detector volume.

As shown in Figure 3, protons with energy lower than 10MeV are stopped by the payload shielding, although they represent a large part of the primary spectrum. It is in good agreement with what as been found by CREAM 96.

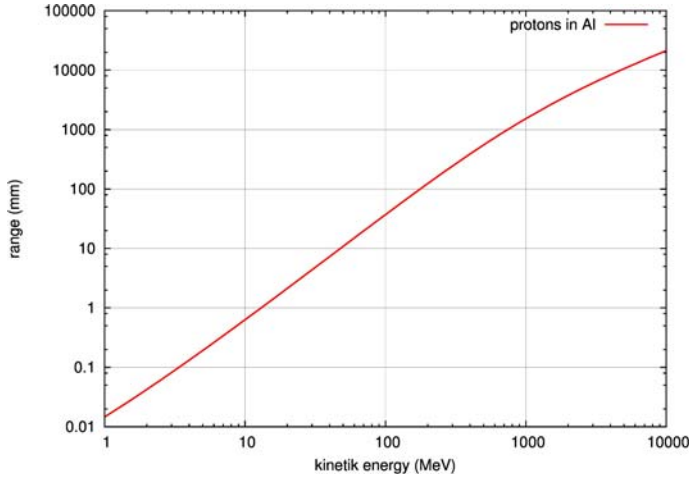

Figure 3: Range of protons energy in Al.

We measure the deposited energy in the NISP detector and the interaction probability of particles as a function of the energy of the incident proton. Both primary and potential generated secondaries are taken into account.

As shown on Figure 4, low energy incident protons have low chances to interact but can deposit a large energy in the HgCdTe detectors, while high energy ones have large chances to interact but will deposit a low energy in detectors.

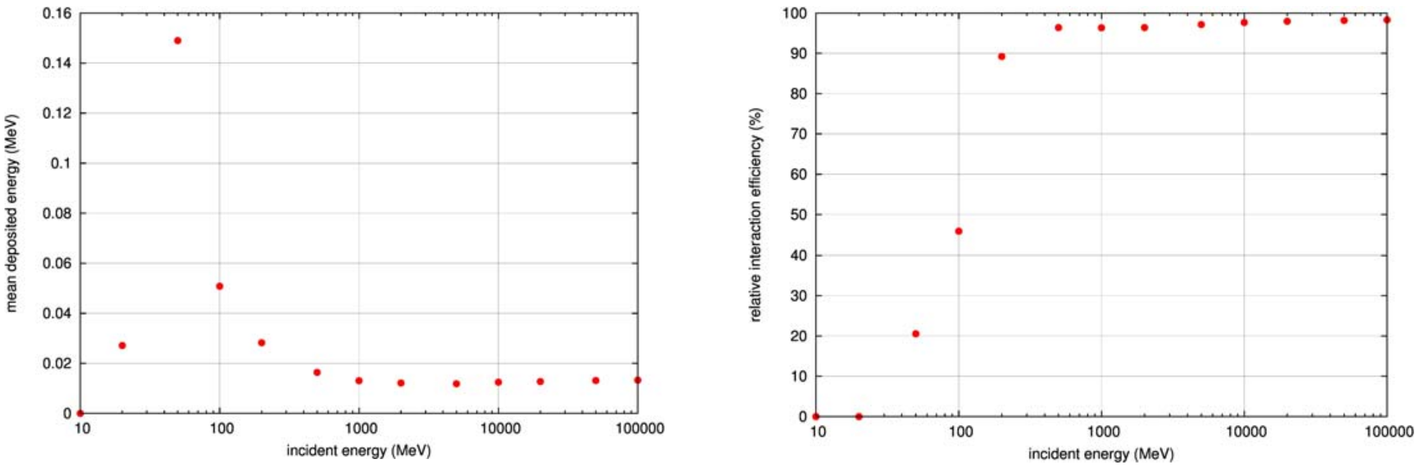

Figure 4: Depositied energy as a function of initial energy of protons at left and interaction probability as a funtion of the intial proton energy at right.

2.2.3 Results

As a final result, we estimate the secondary's production rate as a function of initial energy of protons. As shown by figure 5, a very low rate of protons is able to produce secondaries in the range of the Euclid expected spectrum.

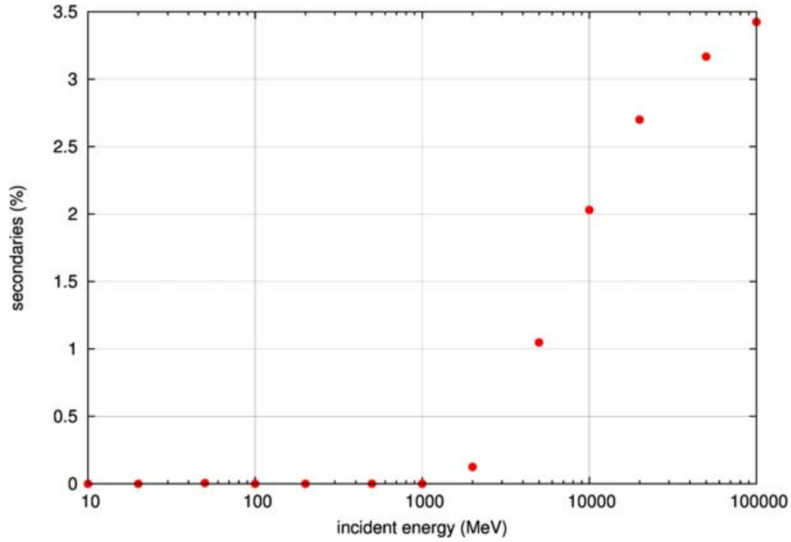

Figure 5: **Secondaries production rate as a function of initial energy of protons.**

Contribution of secondaries in the NISP detector reaches 1% for protons whose incident energy is higher than 5000MeV, whom are in a very low portion in the expected spectrum of Figure 1.

Then from this initial study, we found a very low rate of secondary particles, that will not significantly impact the science images. We will neglect them in the next study.
Anyway we emphasize that the current geometry used in GEANT4 is very crude, and has a lake of information. This should be improved to really believe on the rate production.
This will be pursued in 2 ways:
-Improve the GEANT4 study in the next months with a better geometry, in particular from the telescope.
-Prepare a test in real condition of an engineering detector under a high energy proton beam to tune the GEANT4 results in a realistic way.

3 Simulation of EUCLID NIR detector

We have begun simulating cosmic ray impacts on the detectors using code originally developed by Chris Bebek for SNAP.

3.1 Parameters

We have assumed that the band gap for our HgCdTe is inversely proportional to cutoff wavelength. I.e., that W = 2.61 when the wavelength cutoff is 1.7 microns, (from Fox et al. Fe55 PASP paper), and that it is inversely proportional to the cutoff wavelength in microns.

Others parameters are summarized in Table 1.

parameters	
Pixel size	18.0 microns
Pixel thickness	7 microns
Diffusion	1.7

IPC	2.4
Array size	2048x2048
Exposure time	560s
Record time	1.3 s
Wavelength cut off	2.3 microns

Table 1 : H2rG parameters used in simulation

3.2 Some results

The first indications are that a small percentage of pixels, less than 5% per exposure, will be affected at all by cosmic rays.

An array showing pixels hit in white is shown on Figure 6. All pixels with any electrons from cosmic ray hits are shown in white -- the only values in the image are black and white -- not affected, or affected. Note that care must be taken in interpreting this result, as the image is usually rendered with less than 2048 pixels on the screen.

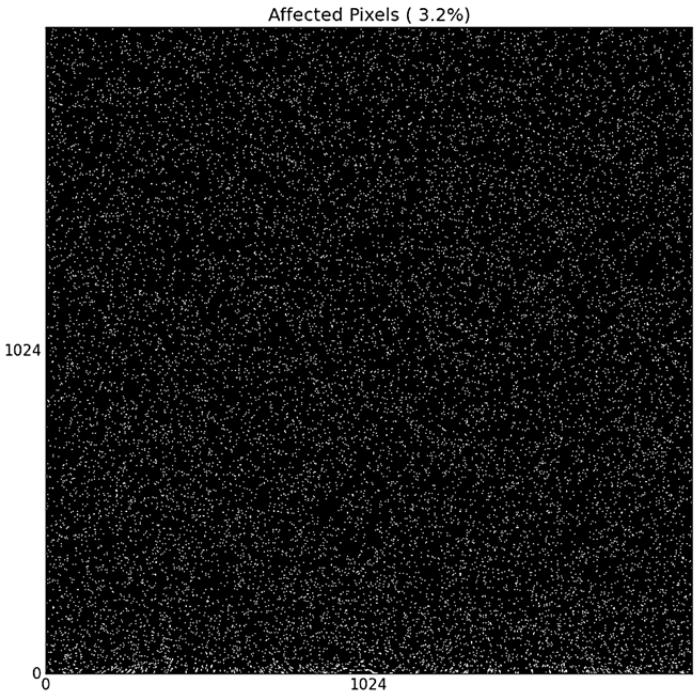

Figure 6: image of an H2RG detector with cosmic in 560s.

We have also confirmed the numbers of electrons generated in a given particle event, and begun to investigate which parts are due to the direct hit, and which parts are affected by diffusion. These are shown in Figure 7. W see that the big peak around > 1000 e is due to primary particles although lower number of electron (from 1 to 1000e) are coming from diffusion + IPC and are simulated under different assumptions.

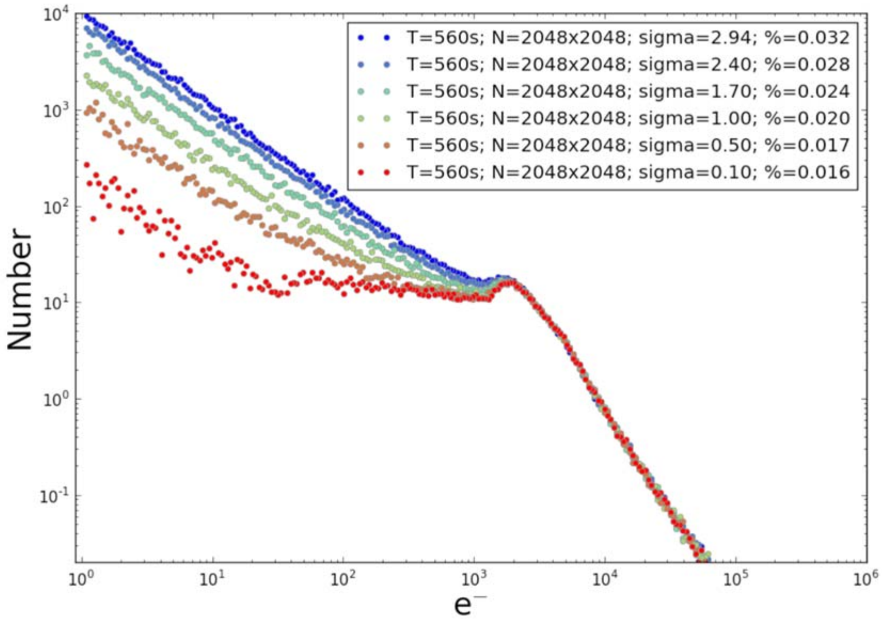

Figure 7: Number of pixel affected by a cosmic ray in one detector in function of the number of electron coming from the cosmic hit in this pixel

4 Simulation of NISP dispersed images with cosmic

4.1 TISP code

TIPS is an image simulator tool which produces dispersed images of an observation of the spectrometry part. The current version of TIPS used in this document, is un update of aXeSIM, image simulator code, developed for HST (**aXeSIM**, Kuemmel et al. 2007 and 2009) and used in previous spectroscopic chain analysis performance of EUCLID (B.Garilli et al.). TIPS is a prototype, which introduce more instrumental effects, is easier to implement in the SGS framework, and is able to simulate the 16 detectors of the spectrometer of EUCLID/NISP. The result of TIPS simulation for a given observation mode is one image for each detector of the focal plan. For more details, see the project web site **http://projects.oamp.fr/projects/tips** and the TIPS description note EUCL-CPPM-WS-S2-TIPS-PROTO-DESC.

4.1.1 The instrument model:

The spectroscopy is based on 4 grisms: 2 in the blue band, 2 in the red band, corresponding to 2 grism line orientations.
-The blue grism (B) covers from 1.1 to 1.457 micron
-The red grism (R) covers from 1.44 to 2 micron

The main parameters used for the instrument model in the simulation are summarized in Table 2 and are, for the moment, closed to what have been used in previous performance analysis.

parameters	values	comment
Dispersion	to 0.54 Angstrom/um (= 9.8 Angstrom/pixel)	constant

Thermal + scattering noise inst	10% zodiacal light	
Thermal + scat scattering telescope	10% zodiacal light	
Gap in X	3mm	
Gap in Y	6 mm	
Pixels array	2040x2040 pixels/detector	4x4 detectors
Pixel size	18um	
Pixel scale	0.3 arcsec	
Total noise in 560s	9 e	Dark 0,1 e/s/pixel
Total throughput	>30%	See perf doc for curve
PSF FWHM	0.45 (B)/0,5''(R)	Double gaussian

Table 2: instrument model parameters used in TIPS simulator

4.1.2 The observational strategy:

The observational strategy is based on the 4 grisms observation sequence in 2 directions and a dithering pattern on the sky as described here:

-560s exposure with NISP/Gblue (0deg)
-shift (100, 50) arcsec
-560s exposure with NISP/Gblue (90deg)
-shift (100, 0) arcsec
-560s exposure with NISP/Gred (0deg)
-shift (100, 0) arcsec
-560s exposure with NISP/Gred (90deg)

4.1.3 The sky and galaxy models

The information needed for each galactic object sources are the position on the sky and the shape parameters (ellipse as in sextractor) with spectra and realistic emission lines. We have used for galaxy catalog, the COSMOS mock catalog (CMC) constructed from the real COSMOS galaxies COSMOS (Jouvel et al. 2009 and Zoubian et al in prep). In addition to the galaxy sources, we simulated the sky background with the zodiacal light model of Aldering et al. 2002.

The science analysis is based on emission line detection, mainly the Hα line. As an example, we shown on **Figure 8** the Hα emission line signal distribution expected in 560 s of exposure with this catalog. We see that the expected number of electron in emission line is less than 1000 e-, which is in general small compared to the cosmic signal.

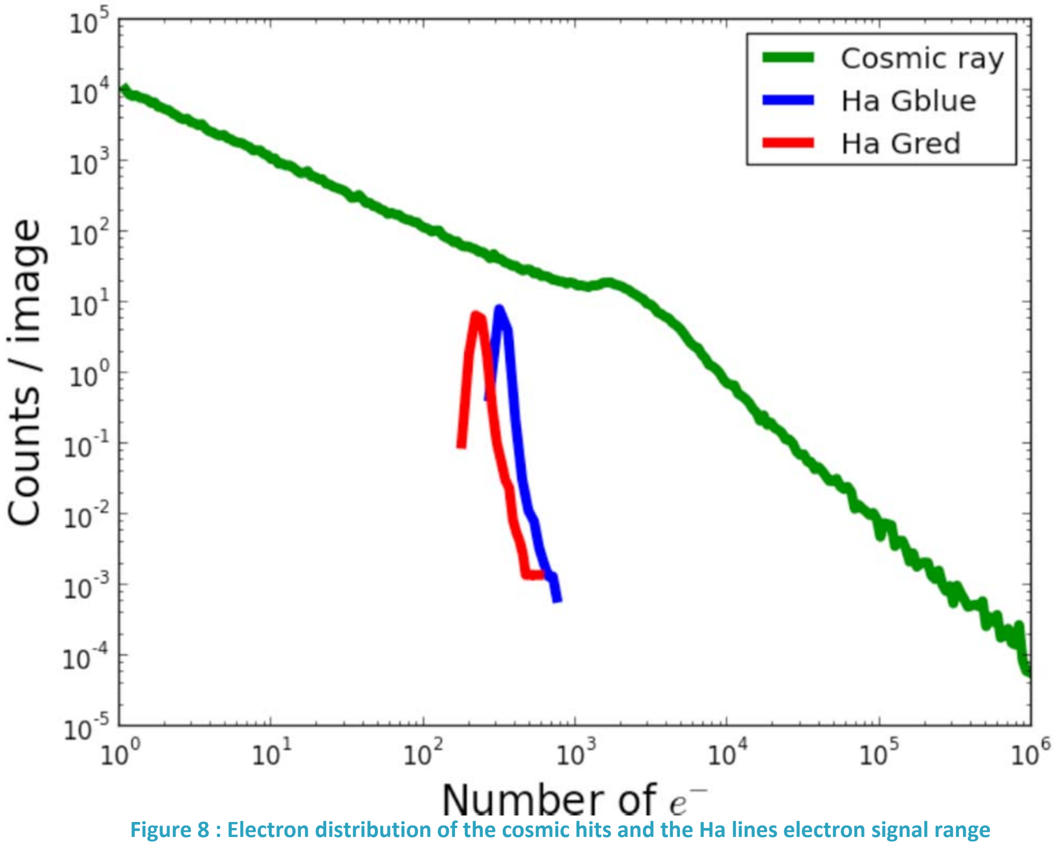

Figure 8 : Electron distribution of the cosmic hits and the Ha lines electron signal range

4.2 Implementation of cosmic rays simulation

The cosmic ray flux was simulated with the code presented in section 3. This code produces images of the cosmic rays on the detector. We implemented then this simulated image on the dispersed image to add cosmic in the pixel.

We have implemented in the code the possibility to simulate a rejection by simply adding an error on the pixel that is affected by a cosmic hit but as the rejection performance numbers are still under evaluation , this case will not be used in this document.

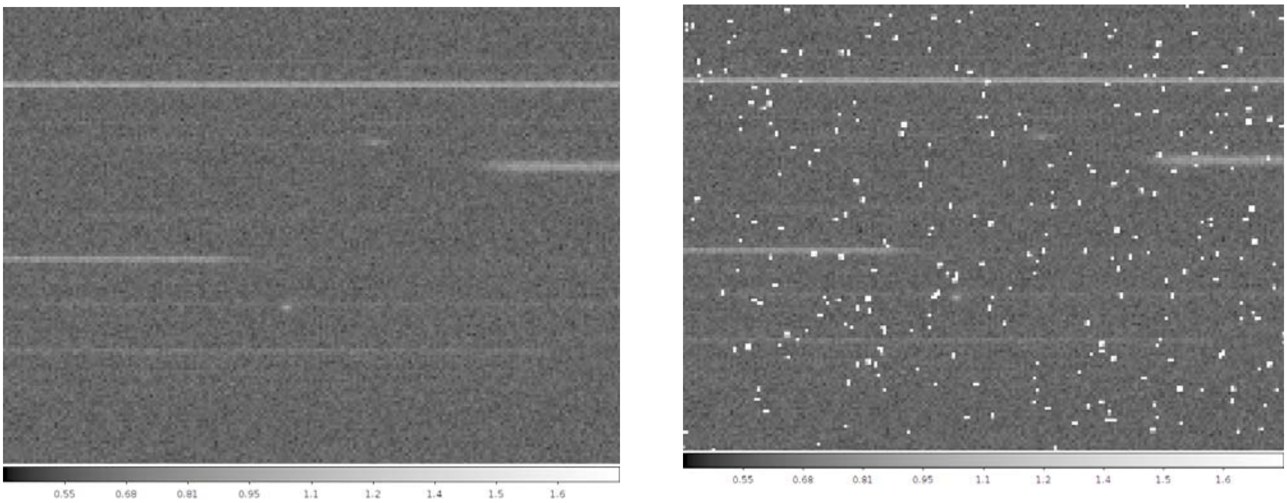

Figure 9: Example of simulation without cosmic at left, and with cosmic at right (zoom of part of the detector).

It appears that the cosmic ray signal is very bright compared to the galactic objects and is very clustered around a central pixel. In general, we observed one very bright pixel which is coming from the primary spectrum and some correlated pixel around linked to diffusion. Because the cosmic hits arrive directly on the image, they are not affected by the PSF and the signal has a very different shape behavior.

5 Science analysis results

We present here a first analysis based on the simulation without cosmic rejection. We have added cosmic information directly in the image. We run the simulation of a full observation of the focal plane to get reliable statistic. We also run a small reduction of the image to subtract the sky background. The current analysis is only based on pixel statistics; the full performance study will be done in the next months with more elaborate tools of extraction and analysis.

5.1 Effects of cosmics

The number of pixels affected by a cosmic ray is quite small: we observe only 3.2% of pixels contaminated by cosmic rays. Moreover, only a part of the contaminated pixels have signal information. **Figure 10** shows that less than 1% of the pixels with a SNR>2 are contaminated and less than 0.5% for the pixels with SNR>3.

Focusing on the Hα line signal, we looked for the lines contaminated by a cosmic in the 3σ area (typically 8 pixels). We found that 15% of Hα lines are contaminated by at least one cosmic ray hit. In 3% of the cases, the central pixel is affected. Matching lines in the two grism orientation images, shows than less than 1% of the Hα lines are contaminated by a cosmic hit using the 2 images.

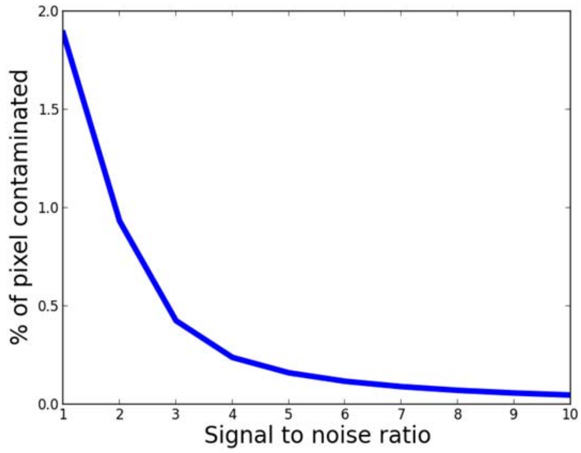

Figure 10 : percentage of pixels contaminated by cosmic rays as function of the signal to noise in the pixel

5.2 Mask the cosmics from blind

Even with a low rate of pixel hits by a cosmic ray, the problem could be not only the signal contamination but also possible fake line produced by a cosmic in the signal range. Most of the cosmic rays in the signal range are due to dispersion and should not be isolated. Then we expect to be able to identify them from the identification of a bright cosmic in an adjacent pixel. We should even be able to apply some correction using comic diffusion model and prior to not lose these pixels.

In this first study, we explore a very simple way to mask the cosmic pixel from blind without any prior. We cut the pixels with a number of electron bigger than the signal range (> 1000 electrons) and cut also all the adjacent pixels. This way to mask is very crude and we expect to have methods able to do something more clever in a short term.

Because of the simplicity of our mask construction, the number of pixel masked is large: 9% of the pixels are masked (and only 3% have a cosmic signal). But as previously, if we focus on the signal pixels in **Figure 11**, less than 3% of pixels with SNR>2 and less than 2% of pixels with SNR>3 are masked.

The most interesting result is that with this very simple mask, less than 0.1% of the pixels are still affected by a cosmic. Then, in this simulation, using the cosmic maximum we can identify most of the pixels affected by the diffusion and we can weight their impact on science.

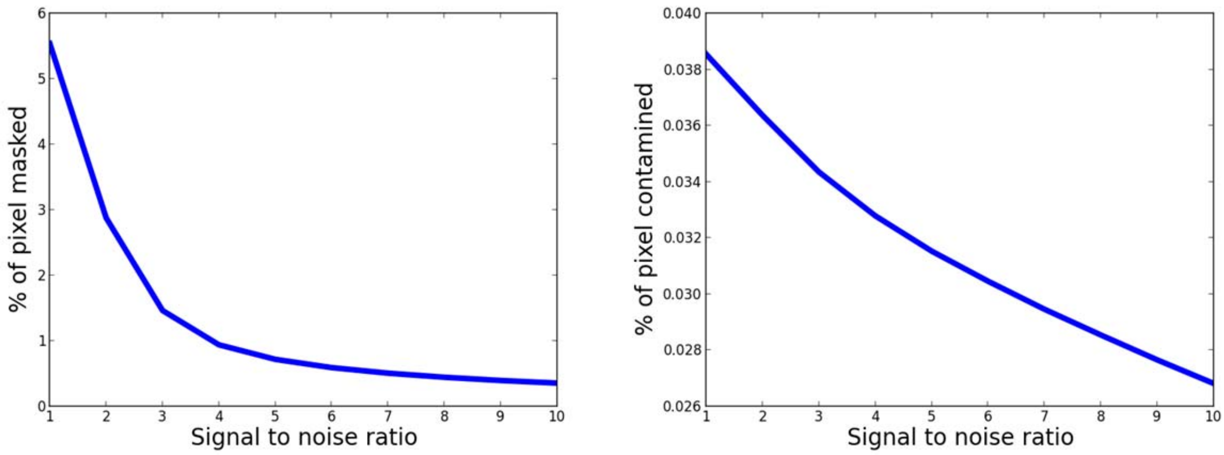

Figure 11 : percentage of masked pixel at left and left contaminated pixel at right as function of the signal to noise cut after

5.3 Conclusion of the science study

In this first simulation of cosmic ray signals on a dispersed science image of the NISP, we have identified that:

- only 3% of Hα line will have a very bright cosmic in and only 1 % of the Ha line are still affected if we use the 2 dithered images. There will be SNR degradation due to diffusion in other cases, that should be investigated to be fully corrected, but we expect this to be recovered in main cases.
- Almost all cosmic rays can be masked on ground (less than 0.1 % still in the images with a crude mask) and this mask will affect only 2% of the pixel with a signal. Here also, if we consider the 2 dithered images, we can reduce the number of lost signal information at < 1%.

6 Conclusion and recommendations to support changes

This study has shown that the NISP images should be mainly affected by energetic proton coming from the galactic flux. Thanks to the detector properties and thickness, these energetic particles will cross the detector with some diffusion and will produce clusters of very bright pixels. The current estimation is that around 3% of the pixel of one detector will be affected and should be removed.

In the science signal, near 10% of Hα emission line will have at least one pixel with cosmic but only 3 % are really affected by a primary one.

It seems easy, if these simulation are realistic, to identify these cosmic rays on ground and to remove them or correct them directly on the image. In this case, we estimate than less than 2% of the signal can be affected which is below the current budget affected on non-operable pixel because of cosmic contamination and then, a cosmic rejection on board is not needed under hypotheses described in this document.

Anyway we emphasize that the secondary particles are not included, because their contribution seems very small, and this should be better studied. Further estimations are under going, including a test plan on a real detector.

We estimate, that the complexity to control the rejection algorithm performance on board and the related complexity of the processing, is not justified currently on a science point of view even if it is an advantage of these detector processing.

We propose to investigate more the on ground rejection solutions without the on board treatment. This can relax the constraint of implementation of the ramp, for example allow to have less points on the ramp in spectroscopy and then, will permit a simplified readout scheme.

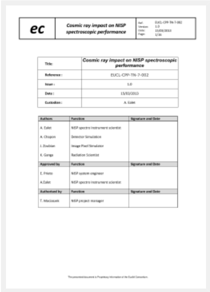

EUCL-CPP-TN-7-002_Cosmic_ray_impact_on_N

EchoSign Document History March 18, 2013

Created:	March 18, 2013
By:	thierry maciaszek (thierry.maciaszek@oamp.fr)
Status:	SIGNED
Transaction ID:	SJYXU92B2Q3462

"EUCL-CPP-TN-7-002_Cosmic_ray_impact_on_NISP_spectroscopic_performance History

Document created by thierry maciaszek (thierry.maciaszek@oamp.fr)
March 18, 2013 - 5:09 PM GMT+1 - 90.50.0.45

Document emailed to Arnaud Chapon (chapon@cppm.in2p3.fr) for signature
March 18, 2013 - 5:12 PM GMT+1

Document viewed by Arnaud Chapon (chapon@cppm.in2p3.fr)
March 18, 2013 - 5:16 PM GMT+1 - 134.158.18.2

Document esigned by Arnaud Chapon (chapon@cppm.in2p3.fr)
March 18, 2013 - 5:16 PM GMT+1 - 134.158.18.2

Document emailed to Julien Zoubian (zoubian@cppm.in2p3.fr) for signature
March 18, 2013 - 5:16 PM GMT+1

Document viewed by Julien Zoubian (zoubian@cppm.in2p3.fr)
March 18, 2013 - 5:52 PM GMT+1 - 195.221.212.151

Document esigned by Julien Zoubian (zoubian@cppm.in2p3.fr)
March 18, 2013 - 5:56 PM GMT+1 - 195.221.212.151

Document emailed to Ken Ganga (ganga@apc.univ-paris7.fr) for signature
March 18, 2013 - 5:56 PM GMT+1

Document viewed by Ken Ganga (ganga@apc.univ-paris7.fr)
March 18, 2013 - 6:27 PM GMT+1 - 134.158.186.76

Document esigned by Ken Ganga (ganga@apc.univ-paris7.fr)
March 18, 2013 - 6:29 PM GMT+1 - 134.158.186.76

Document emailed to Eric prieto (eric.prieto@oamp.fr) for signature
March 18, 2013 - 6:29 PM GMT+1

Document viewed by Eric prieto (eric.prieto@oamp.fr)
March 18, 2013 - 7:25 PM GMT+1 - 88.178.205.128

Document esigned by Eric prieto (eric.prieto@oamp.fr)
March 18, 2013 - 7:26 PM GMT+1 - 88.178.205.128

Document emailed to Anne Ealet (ealet@cppm.in2p3.fr) for signature
March 18, 2013 - 7:26 PM GMT+1

Document viewed by Anne Ealet (ealet@cppm.in2p3.fr)
March 18, 2013 - 7:29 PM GMT+1 - 90.8.184.148

Document esigned by Anne Ealet (ealet@cppm.in2p3.fr)
March 18, 2013 - 7:30 PM GMT+1 - 90.8.184.148

Document emailed to thierry maciaszek (thierry.maciaszek@oamp.fr) for signature
March 18, 2013 - 7:30 PM GMT+1

Document viewed by thierry maciaszek (thierry.maciaszek@oamp.fr)
March 18, 2013 - 7:41 PM GMT+1 - 90.50.0.45

Document esigned by thierry maciaszek (thierry.maciaszek@oamp.fr)
March 18, 2013 - 8:45 PM GMT+1 - 90.50.0.45

Signed document emailed to Arnaud Chapon (chapon@cppm.in2p3.fr), Ken Ganga (ganga@apc.univ-paris7.fr), Anne Ealet (ealet@cppm.in2p3.fr), Julien Zoubian (zoubian@cppm.in2p3.fr), Eric prieto (eric.prieto@oamp.fr) and thierry maciaszek (thierry.maciaszek@oamp.fr)
March 18, 2013 - 8:45 PM GMT+1